Microscopic adjustment of misfit strain and charge segregation in $[Bi_2Sr_2O_4]_{0.51}CoO_2$

Makoto Maki,[1,*] Sho-ichi Takakura,[1] Terukazu Nishizaki,[2] and Fusao Ichikawa[3]
[1]*Department of Physics, Saga University, Saga 840-8502, Japan*
[2]*Department of Electrical Engineering and Information Technology, Kyushu Sangyo University, Fukuoka 813-8503, Japan*
[3]*Department of Physics, Kumamoto University, Kumamoto 860-8555, Japan*
(Received 7 October 2014; revised manuscript received 9 September 2015; published 16 October 2015)

From scanning tunneling microscopy of the misfit-layered cobaltate $[Bi_2Sr_2O_4]_{0.51}CoO_2$ single crystals, we observed structural short corrugations oriented in the direction inclined with respect to the incommensurate axis. Results show that the spatial distribution of the electronic charge density is also modified in relation to the atomic displacement. Our data strongly suggest that the rocksalt structure flexibly mounted on the CoO_2 layer affects the electronic properties of this system.

DOI: 10.1103/PhysRevB.92.165117 PACS number(s): 73.20.−r, 68.37.Ef, 71.28.+d, 61.44.Fw

I. INTRODUCTION

Misfit-layered compounds comprise the stacking of two alternating sublattices, the in-plane periodicities of which are mutually incommensurate along at least one direction [1]. Details of the interfacial effects [2] and chemical bonding mechanisms [3,4] between the adjacent layers remain controversial. For that reason, their electronic properties have attracted wide attention. The misfit cobaltates $[Bi_2M_2O_4]_pCoO_2$, where M = Ba, Sr, or Ca and p is the relative periodicity, consist of a single CoO_2 layer formed by CoO_6 edge-sharing octahedra and four rocksalt (RS)-type layers, as depicted in Fig. 1(a). Similarly to Na ions in Na_xCoO_2, the RS layers are regarded as a charge reservoir. With increasing M^{2+} cation size, the p parameter, being a b-axis ratio b_{CoO_2}/b_{RS}, decreases. The metallicity is enhanced because of increasing effective transferred charges and/or oxygen contents [5,6]. These systems are of wider interest because of their unusual electronic properties such as the low temperature upturn in resistivity (M = Sr) [7], a large negative magnetoresistance (Ca and Sr) [8,9], a weak Curie-Weiss contribution to the susceptibility (Ba) [10], and high thermoelectric power (Ca and Sr) [11].

In the layered cobaltates, the intrinsic properties of the CoO_2 triangular sublattice themselves are of interest because strong correlation effects might play a role in the partially filled Co $3d$ states. However, in Na_xCoO_2, it is believed that Co charge disproportionation occurs in relation to the spatial distribution of Na atoms [12]. Recent angle-resolved photoemission spectroscopy reported a replica Fermi surface in the misfit cobaltates [2,13], indicating that the influence of the adjacent RS layers should be regarded as accounting for the wide variety of unusual properties described above. However, some unresolved issues remain: for example, there is little anisotropy in the electric properties between the commensurate a and incommensurate b axes [14]. Consequently, full consensus on the consequences of the misfit stacking of layers has not been established yet.

To gain insight into these unsolved issues, we conducted scanning tunneling microscopy (STM) measurements of the BiO-terminated surface of $[Bi_2Sr_2O_4]_{0.51}CoO_2$ single crystals. As described in this paper, we present atomic-resolution STM images, which reveal that the misfit causes short-range structural modulations of the RS lattice by correlating with the underlying CoO_2 lattice. Atomic displacements are oriented in the direction inclined with respect to the b axis. The displacements induced the spatial distribution of the charge density. Our experiments demonstrate that the RS structure is flexible and that it should be regarded not as a periodic potential, but as a composite potential made from short-range corrugations.

II. EXPERIMENT

Crystals were grown using a self-flux method starting with powders of Bi_2O_3, $SrCO_3$, and Co_3O_4 mixed in a molar ratio of 3 : 3 : 1. The mixture was transferred to an Al_2O_3 crucible and was melted at 1200 °C and then cooled to room temperature at the cooling rate of 2 °C/h. To equalize the oxygen contents, all crystals were annealed in an argon atmosphere at 600 °C for 48 h. The misfit parameter p was estimated as approximately 0.51 from the electron diffraction pattern shown in Fig. 1(b). The STM measurements were conducted using a commercial LT-STM (Unisoku Co. Ltd.) to which we made some improvements [15]. Samples were introduced into the ultrahigh-vacuum chamber and were then cleaved by knocking off a small post glued on the top surface. Because of the weak van der Waals bonding between the BiO planes, the BiO-terminated surface is clean and stable. All STM images presented here were taken using mechanically sharpened Pt-Ir tips.

III. RESULTS AND DISCUSSION

Figure 1(c) shows a typical constant-height STM image (310 Å on a side) of $[Bi_2Sr_2O_4]_{0.51}CoO_2$ measured at room temperature. The striped pattern is clearly visible as described in previous reports [13]. The stripes extend at an angle of approximately 45° relative to the underlying atomic rows. By considering the lattice constant of BiO ($a \sim 4.9$ Å, $b \sim 5.1$ Å), the atoms observed by STM are either Bi or O. Although the outline of the stripe is not sharp, the periodicity is estimated as approximately 73 Å, which is more than 10 times larger than the lattice constant. The pattern is independent of the polarity of the applied bias, indicating that the striped pattern is of structural origin. In fact, the periodicity is inconsistent

*Corresponding author: mmaki@cc.saga-u.ac.jp

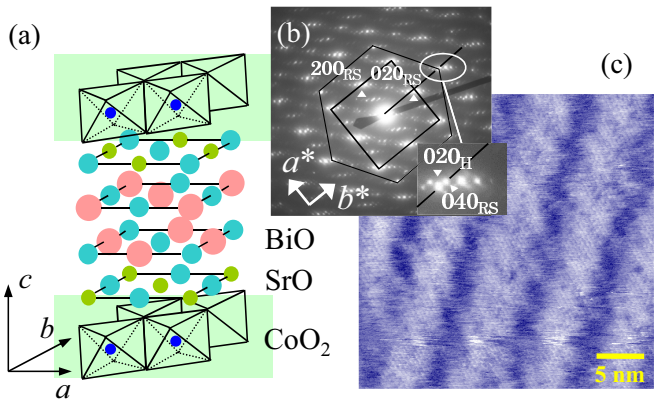

FIG. 1. (Color online) (a) Schematic image of the crystal structure of $[Bi_2Sr_2O_4]_pCoO_2$. (b) Electron diffraction patterns taken with the incident electron beam parallel to the c direction. Subscript H denotes the hexagonal CoO_2 sublattice. (c) Constant-height image (310 Å on a side) taken with $V_{sample} = 80$ mV and $I = 13$ pA.

with the commensurate supercell approximation based on the b_{CoO_2} and b_{RS} parameters. This result agrees well with results of a previous study by Nicolaou *et al.* [13], from which they reported a periodicity of approximately 80 Å.

The fine structure of the pattern can be found as the bias is lowered, as shown in Fig. 2(a) on the same scale as Fig. 1(c). Stripes run from the upper right to the lower left in this image, as shown in Fig. 1(c). The striped pattern is an assembly composed of various sizes of short-range corrugations, the direction of which is misaligned with the stripe direction. In low-bias measurements, another atomic arrangement sometimes appears, depending on the tunneling condition. Figure 2(b) shows a 52 Å × 155 Å constant-current

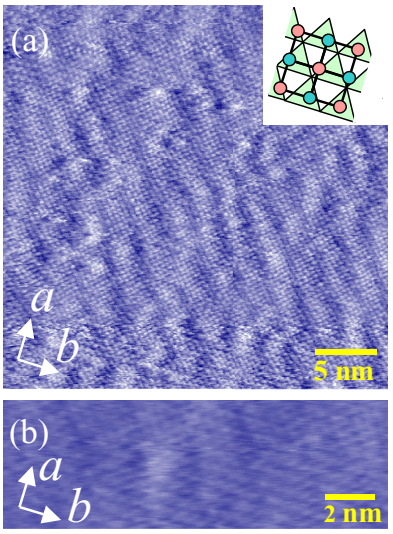

FIG. 2. (Color online) (a) Constant-height image (310 Å on a side) taken on the same surface, as shown in Fig. 1(b). $V_{sample} = -5$ mV, $I = 15$ pA. Schematic of the top view of the BiO plane is shown in the inset. The atomic structure of the underlying CoO_2 layer is also shown as green triangles for simplicity. (b) Different types of constant-current (topographic) images taken on the same surface. 52 Å × 155 Å. $V_{sample} = 10$ mV, $I = 13$ pA.

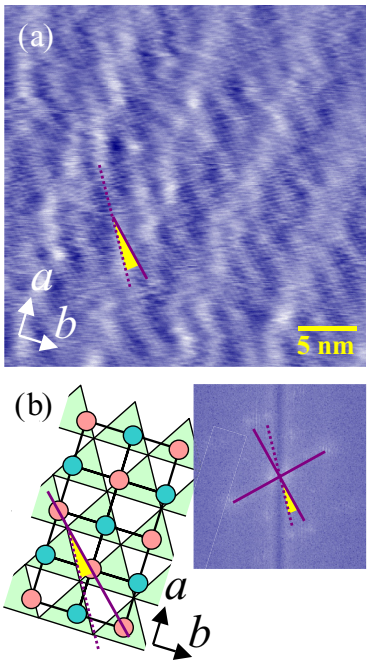

FIG. 3. (Color online) (a) Topographic image taken at a low bias of $V_{sample} = 7$ mV, $I = 15$ pA. The purple line is drawn along the atomic (Bi or O) row, and the dotted one denotes the direction of the corrugations. (b) Schematic of the top view of the BiO plane and the FFT image of the cleaved surface. The FFT spots correspond to the periodicity of either red or blue (Bi or O) atoms. Yellow staining corresponds to the mismatch angle between the RS (BiO) and the CoO_2 lattices.

(topographic) image obtained on the same BiO surface. An effect of the CoO_2 orbitals (triangular-lattice image) is superimposed upon the BiO image. By comparing Figs. 1(c), 2(a), and 2(b), one sees that the stripes are perpendicular to the crystallographic axis, where the lattice vector in the CoO_2 is parallel to that in the RS structure [see schematic drawing in the inset of Fig. 2(a)]. The axis is inclined at an angle of approximately 45° to the atomic (Bi or O) arrangement in Fig. 2(a). The stripes run parallel to the a axis.

We next specifically examine the origin of the short-range corrugations. Figure 3(a) shows a topographic image taken at a low bias of $V_{sample} = 7$ mV. In addition to the stripes, we find the presence of fine structures that are aligned almost in parallel. These short-range corrugations are inclined at an angle of approximately 17° to the atomic line, as shown by yellow staining in Fig. 3(a). This angle of 17° can be interpreted reasonably as a mismatch between the BiO and CoO_2 lattices [see schematic drawing in the left part of Fig. 3(b)]. Actually, in the fast Fourier transform (FFT) image shown in the right-hand part of Fig. 3(b), the spots are spread over a region that corresponds to the mismatch angle, as shown by a dotted line. The FFT pattern clearly reveals the origin of the substructures; i.e., the atoms in the RS structure deform slightly because of interaction with the CoO_2 layer. This provides a reasonable explanation of why the spacing of stripes (approximately 73 Å) has nothing to do with the lattice misfit along the b axis: The misfit strain is adjusted microscopically in the two-dimensional plane.

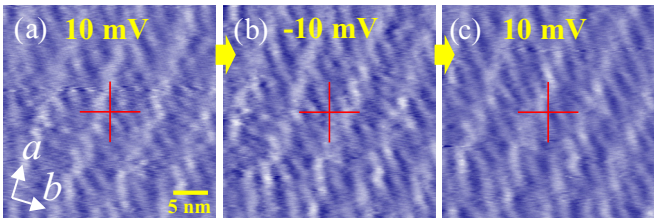

FIG. 4. (Color online) (a)–(c) Sequence of three topographic images (310 Å on a side) taken at positive and negative sample biases ($V_{\text{sample}} = \pm 10$ mV, $I = 15$ pA).

Figures 4(a)–4(c) present a sequence of topographic images acquired under reverse bias conditions. The corrugation image has opposite signs between the filled state and the empty state. This observation is reproducible, which proves that the phase shift is caused not by thermal drift but by the change of bias polarity. Therefore, it is apparent that these short corrugations are *not* merely structural rearrangements. The spatial distribution of the electronic charge density is also modified in relation to the structural rearrangements.

In $[Bi_2Sr_2O_4]_pCoO_2$, the metallicity derives from the CoO_2 layer and is discussed based on the carrier generation because of the change in the average valence of Co ions. An intriguing implication of the present results is that the microscopic adjustment of misfit strain induces inhomogeneous charge distribution in the CoO_2 layer. At room temperature, the dc resistivity exhibits metallic behavior ($d\rho/dT > 0$) in spite of large ρ values exceeding the Mott-Ioffe-Regel criterion, $k_F l \sim 1$ [16], where k_F and l respectively denote the Fermi momentum and the mean free path. Assuming that the nonequivalent Co sites are generated by the adjacent structures as discussed for Na atoms in Na_xCoO_2, this bad-metal behavior can be understood as the percolation of charge carriers through the contact of the charge-rich (or charge-transferable) portions. Unusual behavior such as negative magnetoresistance seems to support the electron flow in narrow metallic channels [17].

Actually, the striped pattern induced by the misfit strain is temperature dependent. Figure 5(a) shows a constant-height image taken on the same sample as in Fig. 3 at 77 K. The striped pattern does appear. The finer structures are also visible in the lower part of Fig. 5(a). Even at the low temperature, the striped pattern results from fine tuning of the position of the corrugations. However, the stripe interval is estimated as 62–64 Å, which is markedly shorter than that at room temperature. This finding was confirmed in other samples. In Fig. 5(b), we present a constant-height image of the other crystal, together with the atomic arrangement obtained on the same surface (see the inset). At 77 K, we found that the stripes comprise short-range corrugations that are misaligned by approximately 10° with respect to the atomic line [see yellow staining in Fig. 5(b)]. These results indicate that the lattice deformations depend on the temperature and that the RS structure is mounted flexibly on the CoO_2 layer. Because of the close relation with the structural rearrangements, it is natural to consider that the internal charge distribution is also altered by changing the temperature. Therefore, we believe that the unusual temperature dependence in electrical transport properties can be understood in terms of the charge segregation under

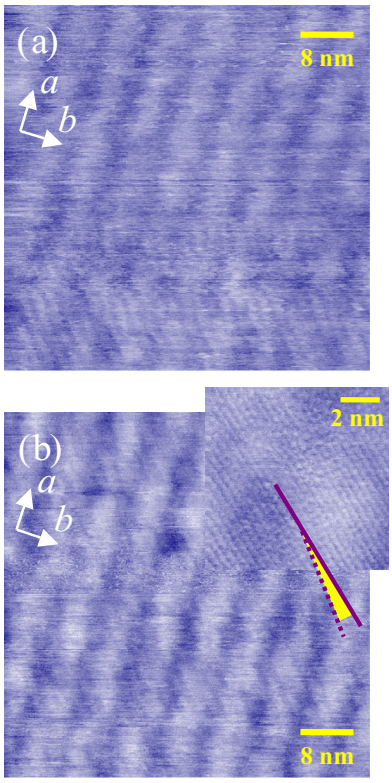

FIG. 5. (Color online) (a) Constant-height image (530 Å on a side) taken at 77 K. $V_{\text{sample}} = 20$ mV, $I = 20$ pA. (b) Constant-height image (530 Å on a side) taken at 77 K. $V_{\text{sample}} = 40$ mV, $I = 20$ pA. Inset: Atomic image obtained on the same surface. 88 Å on a side, $V_{\text{sample}} = 14$ mV, $I = 30$ pA, 77 K. The purple line is drawn along the atomic row in the inset; the dotted line denotes the direction of the corrugations in the main figure.

the composite potential made from short-range corrugations. However, further studies must explore this point in greater detail. We will attempt to investigate the bulk properties which reflect the presence of electronic inhomogeneity, and the difference of thermal expansion between the individual layers. Moreover, at present, we do not know how satellite reflections in the electron diffraction pattern [Fig. 1(b)] or the previously reported modulations relate to the short-range corrugations [18–21]. Therefore, low-temperature electron diffraction studies are also being conducted now.

IV. SUMMARY

In conclusion, we conducted scanning tunneling microscopy measurements of the BiO surface of $[Bi_2Sr_2O_4]_{0.51}CoO_2$. Results show that relaxation of the misfit strain drives the self-assembled formation of short-range corrugations in the charge distribution as well as in the crystal structure. The exotic electronic properties of this material are probably attributable to the inhomogeneous charge state in the CoO_2 layer. Our findings suggest that, in a natural superlattice structure with alternate stacking of two incommensurate structures, self-organized charge segregation possibly occurs microscopically because of the effects of the misfit strains.

ACKNOWLEDGMENTS

This work was partly supported by the Advanced Characterization Platform of the Nanotechnology Platform Japan. We are grateful to Y. Tomokiyo and E. Tanaka of Kyushu University for their helpful support in transmission electron microscopy analysis. This work was supported financially by the Takahashi Industrial and Economic Research Foundation.

[1] G. A. Wiegers, Prog. Solid State Chem. **24**, 1 (1996).
[2] H. W. Ou, J. F. Zhao, Y. Zhang, B. P. Xie, D. W. Shen, Y. Zhu, Z. Q. Yang, J. G. Che, X. G. Luo, X. H. Chen, M. Arita, K. Shimada, H. Namatame, M. Taniguchi, C. M. Cheng, K. D. Tsuei, and D. L. Feng, Phys. Rev. Lett. **102**, 026806 (2009).
[3] M. Kalläne, K. Rossnagel, M. Marczynski-Bühlow, L. Kipp, H. I. Starnberg, and S. E. Stoltz, Phys. Rev. Lett. **100**, 065502 (2008).
[4] E. Kabliman, P. Blaha, and K. Schwarz, Phys. Rev. B **82**, 125308 (2010).
[5] V. Brouet, A. Nicolaou, M. Zacchigna, A. Tejeda, L. Patthey, S. Hébert, W. Kobayashi, H. Muguerra, and D. Grebille, Phys. Rev. B **76**, 100403(R) (2007).
[6] S. Hébert, W. Kobayashi, H. Muguerra, Y. Bréard, N. Raghavendra, F. Gascoin, E. Guilmeau, and A. Maignan, Phys. Status Solidi A **210**, 69 (2013).
[7] T. Yamamoto, K. Uchinokura, and I. Tsukada, Phys. Rev. B **65**, 184434 (2002).
[8] A. Maignan, S. Hébert, M. Hervieu, C. Michel, D. Pelloquin, and D. Khomskii, J. Phys. Condens. Matter **15**, 2711 (2003).
[9] W. Kobayashi, H. Muguerra, S. Hébert, D. Grebille, and A. Maignan, J. Phys. Condens. Matter **21**, 235404 (2009).
[10] M. Hervieu, A. Maignan, C. Michel, V. Hardy, N. Créon, and B. Raveau, Phys. Rev. B **67**, 045112 (2003).
[11] A. Maignan, W. Kobayashi, S. Hébert, G. Martinet, D. Pelloquin, N. Bellido, and Ch. Simon, Inorg. Chem. **47**, 8553 (2008).
[12] H. Alloul, I. R. Mukhamedshin, T. A. Platova, and A. V. Dooglav, Europhys. Lett. **85**, 47006 (2009).
[13] A. Nicolaou, V. Brouet, M. Zacchigna, I. Vobornik, A. Tejeda, A. Taleb-Ibrahimi, P. Le Fèvre, F. Bertran, C. Chambon, S. Kubsky, S. Hébert, H. Muguerra, and D. Grebille, Europhys. Lett. **89**, 37010 (2010).
[14] T. Fujii, I. Terasaki, T. Watanabe, and A. Matsuda, Jpn. J. Appl. Phys. **41**, L783 (2002).
[15] M. Maki, T. Nishizaki, K. Shibata, and N. Kobayashi, Phys. Rev. B **72**, 024536 (2005).
[16] The maximum metallic resistivity ρ_M for $k_F l \sim 1$ is estimated as $\rho_M \sim 4$ mΩ cm, using the two-dimensional Boltzmann formula $\rho_{ab} = hc/(e^2 k_F l)$ and the c-axis length of approximately 1.5 nm. We obtained $\rho_a \sim 15.6$ mΩ cm and $\rho_b \sim 17.7$ mΩ cm at room temperature, which agrees with other published results.
[17] S. B. Arnason, S. P. Herschfield, and A. F. Hebard, Phys. Rev. Lett. **81**, 3936 (1998).
[18] M. Hervieu, Ph. Boullay, C. Michel, A. Maignan, and B. Raveau, J. Solid State Chem. **142**, 305 (1999).
[19] H. Leligny, D. Grebille, O. Pérez, A. C. Masset, M. Hervieu, and B. Raveau, Acta Crystallogr. Sect. B **56**, 173 (2000).
[20] K. Yubuta, S. Begum, Y. Ono, Y. Miyazaki, and T. Kajitani, Jpn. J. Appl. Phys. **45**, 4159 (2006).
[21] M. Hervieu and C. Michel, J. Mater. Chem. **17**, 1743 (2007).